UC Irvine
UC Irvine Previously Published Works

Title

Use of labeled tomato lectin for imaging vasculature structures

Permalink

Journal

Histochemistry and Cell Biology, 143(2)

ISSN

0948-6143

Authors

Robertson, Richard T
Levine, Samantha T
Haynes, Sherry M
et al.

Publication Date

2015-02-01

DOI

10.1007/s00418-014-1301-3

Peer reviewed

Use of labeled tomato lectin for imaging vasculature structures

Richard T. Robertson, Samantha
T. Levine, Sherry M. Haynes, Paula
Gutierrez, Janie L. Baratta, Zhiqun Tan
& Kenneth J. Longmuir

Springer

SHORT COMMUNICATION

Use of labeled tomato lectin for imaging vasculature structures

**Richard T. Robertson · Samantha T. Levine ·
Sherry M. Haynes · Paula Gutierrez · Janie L. Baratta ·
Zhiqun Tan · Kenneth J. Longmuir**

Abstract Intravascular injections of fluorescent or biotinylated tomato lectin were tested to study labeling of vascular elements in laboratory mice. Injections of *Lycopersicon esculentum* agglutinin (tomato lectin) (50–100 μg/100 μl) were made intravascularly, through the tail vein, through a cannula implanted in the jugular vein, or directly into the left ventricle of the heart. Tissues cut for thin 10- to 12-μm cryostat sections, or thick 50- to 100-μm vibratome sections, were examined using fluorescence microscopy. Tissue labeled by biotinylated lectin was examined by bright field microscopy or electron microscopy after tissue processing for biotin. Intravascular injections of tomato lectin led to labeling of vascular structures in a variety of tissues, including brain, kidney, liver, intestine, spleen, skin, skeletal and cardiac muscle, and experimental tumors. Analyses of fluorescence in serum indicated the lectin was cleared from circulating blood within 2 min. Capillary labeling was apparent in tissues collected from animals within 1 min of intravascular injections, remained robust for about 1 h, and then declined markedly until difficult to detect 12 h

after injection. Light microscopic images suggest the lectin bound to the endothelial cells that form capillaries and endothelial cells that line some larger vessels. Electron microscopic studies confirmed the labeling of luminal surfaces of endothelial cells. Vascular labeling by tomato lectin is compatible with a variety of other morphological labeling techniques, including histochemistry and immunocytochemistry, and thus appears to be a sensitive and useful method to reveal vascular patterns in relationship to other aspects of parenchymal development, structure, and function.

Introduction

Most cells and tissues of vertebrates rely on the vascular system to deliver oxygen, nutrients, and regulatory molecules, and also to carry away byproducts of cellular metabolism. Hence, an understanding of the organization and structure of vasculature elements is essential for an understanding of the development, structure, and function of virtually any organ of the body. A sensitive and reliable technique for visualizing the blood vessels would be highly useful for these studies.

Immunocytochemical techniques have been used to identify vascular elements, primarily the use of antibodies against components of endothelial cells including von Willebrand factor (Baluk and McDonald 2008), CD31 (or PECAM-1) (Newman and Albelda 1992; Baluk and McDonald 2008; Lokmic and Mitchell 2011), or CD34 (Fina et al. 1990). Lectins are carbohydrate-binding

R. T. Robertson (✉) · S. T. Levine · P. Gutierrez · J. L. Baratta
Department of Anatomy and Neurobiology, School of Medicine, University of California, Irvine, CA 92697-1280, USA
e-mail: rtrobert@uci.edu

R. T. Robertson · K. J. Longmuir
The Chao Family Comprehensive Cancer Center, University of California, Irvine, CA 92697-1280, USA

S. M. Haynes · K. J. Longmuir
Department of Physiology and Biophysics, University of California, Irvine, CA 92697-4560, USA

Z. Tan
The M.I.N.D. Institute, University of California, Irvine, CA 92697-1280, USA

proteins, distinct from antibodies, enzymes, and transport proteins (Barondes 1988). Lectins can be tagged fluorescently or with biotin, and have been used to label vascular elements in fixed tissue sections, through their binding to carbohydrate components of the endothelial plasmalemma (Nag 1985; Jilani et al. 2003; Baratta et al. 2009). Others have used intravascular injections of one or more of several different lectins to label certain vascular elements (Alroy et al. 1987; Debbage et al. 1998; Hashizume et al. 2000; Lee et al. 2002; Gee et al. 2003; Lokmic and Mitchell 2011). Results reported thus far indicate wide variation in the efficacy of vascular labeling of different lectins, and that tomato lectin may provide the best labeling of central nervous system vasculature (Alroy et al. 1987; Debbage et al. 1998; Jilani et al. 2003; Lokmic and Mitchell 2011; Smolkova et al. 2001). The purpose of this project was to test the utility of intravenous injection of tomato lectin (Nachbar et al. 1980) to visualize elements of the vascular system in several different organs.

Methods

Adult mice, of the C3H ($n = 15$), CD-1 ($n = 2$), or BALB/c ($n = 4$) strains, were used in these experiments. Mice were purchased from Charles River Laboratories (Hollister, CA) and maintained in the UC Irvine satellite vivarium with a 12–12 light cycle. All experiments were approved by local Institutional Animal Care and Use Committee and adhered to NIH guidelines.

Mice were lightly sedated with intraperitoneal (IP) injections of ketamine (70 mg/kg) and xylazine (10 mg/kg). Mice were given injections of 5 ml normal saline IP, to assure hydration and normal fluid levels. A depilatory (Veet; Reckiff Benckisen, Parsippany, NJ) was applied to the tail to remove fur. Body temperature was maintained by a heating pad, and the tail was warmed to ~40 °C by immersion in warm water.

Lycopersicon esculentum agglutinin (LEA, tomato lectin; Vector Labs, Burlingame, CA) was injected intravascularly in an attempt to label vascular elements. Fluorescent Dylight 488 lectin (λ Ex 493 nm; λ Em 518 nm) was used most commonly, but Dylight 594 lectin (λ Ex 592 nm; λ Em 617 nm) and biotinylated lectin also were used. The biotinylated lectin was used for bright field microscopy. Formulations were injected at room temperature, either at full strength (1 mg/ml) as supplied by the manufacturer (Vector Labs) or diluted 1:1 with sterile normal saline.

Injections of 50–200 µg tomato lectin were made using an insulin syringe equipped with a 30-G needle. In one group of mice ($n = 12$), injections were made into the proximal tail vein. At times ranging from 3 min to 2 days following the injection, animals were deeply anesthetized with sodium pentobarbital (50 mg/kg; IP) and perfused through the heart using a MasterFlex electric pump (Cole Parmer, Chicago, IL) connected to a 26-G needle, set at a pumping rate of 5 ml/min. Perfusion fluids included 10 ml sodium-phosphate (Na-PO$_4$)-buffered saline (PBS) to clear the liver of blood, followed by 20 ml of Na-PO$_4$ buffered 4 % paraformaldehyde.

In another group of mice ($n = 4$), the animals were deeply anesthetized (sodium pentobarbital; 50 mg/kg; IP), the thoracic cavity opened, and 100 µg of tomato lectin in 100 µl volume injected directly into the left ventricle of the heart, over a period of approximately 30 s. The heart continued to beat for approximately 1 min following the injection, and then, the animal was perfused through the left ventricle with 10 ml PBS followed by 20 ml PBS 4 % paraformaldehyde, as described above.

A third group of animals ($n = 3$) was anesthetized as described above and perfused through the left ventricle with 10 ml PBS. As the PBS was being pumped through the vascular system, 100 µg tomato lectin was slowly (over 30 s) injected into the left ventricle of the heart, to be pumped through the vascular system along with the PBS.

An additional mouse was purchased from Charles River (Hollister, CA) with an indwelling catheter in the jugular vein. This animal was sedated with the ketamine–xylazine mixture. A mixture of 100 µg of Dylight 488 tomato lectin in 100 µl volume along with 100 µl of a suspension containing Bodipy-TRX-labeled (λ Ex 589 nm; λ Em 617 nm) long-circulating liposomes (Longmuir et al. 2009) was injected through a port into the jugular vein. Blood samples from the tail were collected at 15 and 30 s, and 1, 2, 3, 4, and 5 min following injection, using Sarstedt Microvette CB300 capillary blood collection tubes (Sarstedt, Newton, NC). Tubes were centrifuged at $4,000 \times g$ for 5 min. Then, 3 µl of plasma was diluted to 1.0 ml with PBS, and the 488 Dylight and the Bodipy-TRX emission spectra recorded digitally using a Varian Eclipse spectrofluorometer. The rate of clearance of the long-circulating liposomes is known from our previous work (Longmuir et al. 2006, 2009; Robertson et al. 2008), and this slow rate of blood clearance (approximately 5 %/h) of red-labeled liposomes was used as a reference against which the measurements of the green Dylight 488-labeled lectin were compared.

Following perfusion fixation, tissues including brain, kidney, liver, spleen, skin, heart, muscle, and intestine were collected and placed into 4 % paraformaldehyde for overnight fixation at 4 °C. The following day, tissues were transferred to a solution of 30 % sucrose in PBS, for cryoprotection.

Tissues for light microscopy were cut either for thin (10–12 µm) sections, using a Reichert-Jung Cryocut 180 or Microm HM 505E cryostat, and mounted directly onto slides (Superfrost Plus slides; Fisher Scientific, Pittsburgh,

PA) or for thick (25–100 μm) sections using a vibratome, and placed in PBS in 24-well plates. Care was taken to protect tissue from exposure to overhead room fluorescent light as much as possible. Cryostat sections were cover-slipped using Vectashield (Vector Labs, NY) with DAPI (4′,6-diamidino-2-phenylindole), as a fluorescent nuclear stain; vibratome sections were mounted on slides and coverslipped.

Sections from animals injected with the biotinylated lectin were processed using the Elite ABC Kit (Vector Labs; Burlingame, CA) with the ImmPACT DAB peroxidase substrate kit.

In two cases, tissues were taken from animals processed by the Edu technique to label sites of recent cell division. The Edu (5-ethynyl-2′-deoxyuridine, a nucleoside analog of thymidine) (Click-IT; Life Technologies, Grand Island, NY) was prepared in saline at 2.5 mg/ml and administered by IP or IV injections at 250 μg/100 μl to a 20- to 25-g mouse. Following post-injection survival times ranging from 3 h to 7 days, animals were lightly anesthetized with ketamine–xylaxine as described above, and injected with 488 Dylight tomato lectin into the tail vein. After 3–5 min, animals were deeply anesthetized with sodium pentobarbital (50 mg/kg; IP) and perfused through the heart with a PBS flush followed by 4 % paraformaldehyde, as described above. Incorporated Edu leading to cell labeling was detected using a Click-IT Edu kit, as described by the manufacturer (Life Technologies, Grand Island, NY). The red (Alexa Fluor 594; λ Ex 590 nm; λ Em 615 nm) fluorphore was used.

Selected sections were also processed for immunocytochemistry. Antibodies included (1) a fluorescein-labeled antibody against albumin (Bethyl Labs, Montgomery, TX; raised in rat; dilution 1:500), (2) a rat monoclonal antibody CD34 (Vector Labs, Burlingame, CA; dilution 1:1,000), and (3) a rat monoclonal antibody to CD31 (Dianova Hamburg DE; dilution 1:3,000). Cryostat cut sections mounted on slides were rinsed in Tris buffer (0.1 M, pH 7.4) for 5 min and then processed for nonspecific blocking in 3 % normal goat serum for 1 h. Primary antibodies were diluted in Tris buffer, at dilutions presented above, and incubated overnight in darkness and at room temperature. The following day, slides were rinsed 3× in Tris buffer. The tissue processed for the albumin antibody required no further processing. Tissues processed with the CD34 and CD31 antibodies were incubated in a secondary antibody (anti-rabbit or anti-rat) for 2 h at room temperature in darkness. Secondary antibodies were labeled with Alexa Fluor 594 (λ Ex 592 nm; λ Em 617 nm). After incubation in the secondary antibody, slides were rinsed three times for 10 min each in Tris buffer and then coverslipped with Vectashield (Vector Labs), which included DAPI, an ultraviolet fluorescent nuclear stain useful for studying nuclear morphology and tissue architecture.

Sections were examined under a Nikon fluorescence microscope, equipped with a D5 Nikon digital camera. Manual controls for brightness and exposure times were used to maintain consistency in image capture to facilitate comparison of labeling between animals and techniques. Images were imported into Photoshop for placement into figure plates.

In two cases of animals receiving injections of biotin-labeled lectin, tissue processed for biotin was prepared for electron microscopy. This tissue was post-fixed in 4 % paraformaldehyde and 0.5 % glutaraldehyde, and cut on a vibratome at 50 μm. Sections were placed in 1 % osmium tetroxide for 30 min, and then embedded in epoxy, cut at 800 nm, and stained with uranyl acetate and lead citrate to enhance contrast. These stained sections were inspected on a JEOL JEM 1400 electron microscope equipped with a Gatan digital camera.

Results

Examples of vascular labeling

Examples of labeling following injections into the tail vein of mice of 100 μg of tomato lectin in 100 μl volume, with post-injection survival times of 3–5 min, are presented in Fig. 1. Figure 1a presents a fluorescent image from a transverse section through the forebrain, cut with a vibratome at 50 μm thickness. The green fluorescent tomato lectin has labeled many small vessels, apparently capillaries, and a few larger vessels (indicated by arrows), that may be venules. This dense pattern of vascular labeling was present throughout the brain. Figure 1b presents a section from liver, cut by a cryostat at 12 μm thickness. The green tomato lectin again labels vascular elements, which appear to be the rich sinusoidal capillary plexus of the liver, and was seen throughout the liver. The photomicrograph in Fig. 1c presents a cryostat section of kidney cortex, showing several lectin-labeled glomeruli (g) and associated afferent arterioles (aa) and intralobular arteries (ila).

Addition of the nuclear label DAPI, appearing blue when viewed under ultraviolet fluorescence optics, allows the vascular structures to be seen in context of the local tissue architecture. For example, Fig. 1d presents a 25-μm vibratome section from pyriform cortex of the brain. The vascular elements again are clearly visible in green fluorescence, while the densely cellular cortical layer III is visible in blue. Similarly, Fig. 1e presents a 12-μm cryostat section of liver, as seen under medium power magnification. In this case, the DAPI clearly shows the nuclei of hepatocytes and other cells. Because the sinusoidal capillaries of the liver are formed by a discontinuous endothelial layer (Wisse
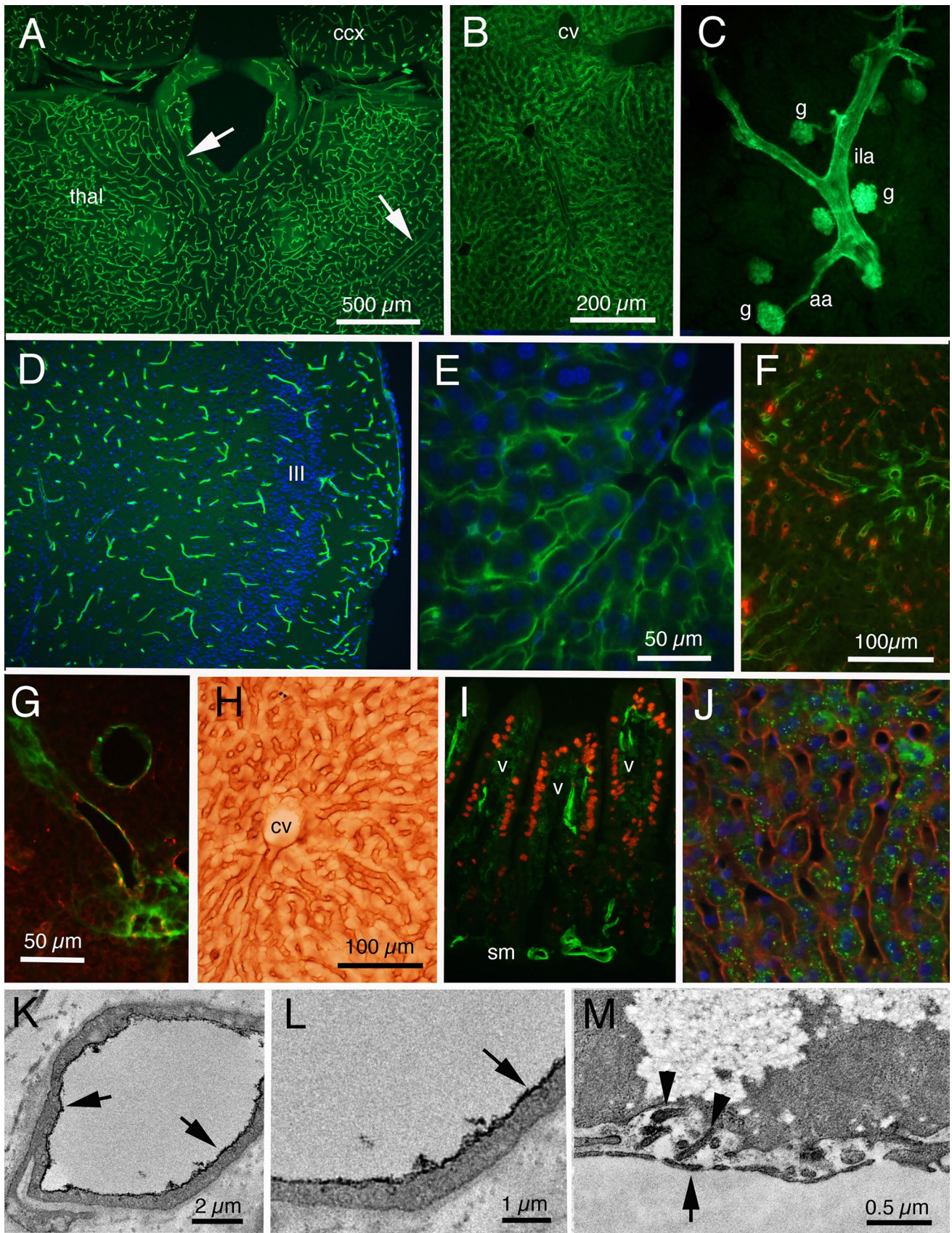
◄**Fig. 1** Fluorescence and bright field photomicrographs showing examples of lectin labeling of vasculature. **a** Low-magnification green fluorescence image of dorsal diencephalon of brain; 50 μm vibratome section. *ccx* cingulate cortex, *thal* thalamus; *arrows* indicate larger vessels. **b** Medium magnification image of liver; 12-μm cryostat section. *cv* central venule. **c** Kidney cortex, showing an intralobular arteriole (ila), afferent arterioles (aa), and several glomeruli (g); 12-μm crystat section. **d** Green lectin staining of pyriform cortex of brain, with DAPI blue stain of nuclei showing cortical cell nuclei (III: cortical layer 3); 50-μm vibratome section. **e** Medium power photomicrograph of green lectin-labeled sinusoidal capillaries of liver, along with DAPI-stained nuclei; 12-μm cryostat section. **f** Green lectin-stained sinusoidal capillaries of liver, with additional red-labeled 30-nm fluorescent microspheres that also label endothelial cells; 12-μm cryostat section. **g** Green lectin labeling combined with red CD31 immunoreactivity of endothelial cells in a Hepa-129 liver tumor; 12-μm cryostat section. **h** Medium power right field photomicrograph showing biotin-labeled lectin labeling of sinusoidal capillaries of liver; 25-μm vibratome section. **i** Green lectin labeling of vascular structures in villi from a section of small intestine. Red Edu labeling of recently divided epithelial cells; 12-μm cryostat section. Lectin-labeled vessels are seen in submucosa (sm) and in villi (v). **j** Medium power photomicrograph of red lectin-labeled sinusoidal capillaries of liver, along with green fluorescence labeling of albumin within hepatocytes and with blue DAPI-stained nuclei; 12-μm cryostat section. **k** Low-magnification electron micrograph showing biotin lectin labeling of the luminal surface (*arrows*) of endothelium of a small vessel (possibly a capillary or venule) from perimysium of skeletal muscle. **l** Higher magnification of a portion of the image in **k**; *arrow* indicates dark biotin lectin labeling of the luminal surface of endothelium. **m** Electron micrograph showing biotin lectin labeling of endothelium (*arrow*) and of hepatocyte microvilli (*arrow heads*) associated with the space of Disse in liver. *Calibration bars* as indicated; *calibration bar* in **b** = 200 μm for **b**, **c**, and **d**; *bar* in **h** = 100 μm for **h**, **i**, and **j**

1970), some of the lectin can be seen to have leaked from the sinusoids to label some intercellular material.

The pattern of labeled lectin is similar to the pattern displayed by other methods of labeling capillaries. For example, Fig. 1f presents a photomicrograph taken from a section of liver from a mouse that received a tail vein injection of the green-labeled lectin along with red (rhodamine)-labeled fluorescent latex microspheres, of 20 nm diameter. These small latex microspheres are known to be taken up by capillary endothelial cells of the liver (Baratta et al. 2009). The green and red labels display similar patterns, indicating co-labeling of the liver's sinusoidal capillaries. Further, Fig. 1g presents a photomicrograph of an experimental Hepa-129 tumor from a mouse that was processed for red-labeled CD31 (or PECAM-1, a marker for endothelial cells) along with the intravenously administered green tomato lectin. The red CD31 immunoreactivity overlaps the green lectin binding, indicating both labels are marking endothelial cells.

The pattern of vascular labeling was essentially identical irrespective of the particular label attached to the tomato lectin. Figure 1h shows the pattern of tomato lectin-labeled liver vasculature when demonstrated using the

avidin–biotin process. The biotin reaction allows the tissue to be viewed under bright field illumination as seen here; the pattern of labeling of sinusoidal capillaries is similar to the patterns presented above in Fig. 1b, e. Further, the red (Dylight 594)-labeled lectin resulted in the same patterns of vascular labeling as the green (Dylight 488).

Lectin labeling of vascular structures also can be seen in the small intestine, as shown in Fig. 1i. In this case, the mouse was treated systemically with Edu 4 days prior to the intravenous injection of tomato lectin and the subsequent vascular perfusion. The red Edu label shows the position of nuclei of epithelial cells covering mid and distal portions of the intestinal villi (v), while the green lectin reveals vascular elements in the submucosal layer (sm) and in individual villi (v).

Visualizing vascular elements by intravenous application of tomato lectin also is compatible with immunohistochemical techniques. For example, Fig. 1j presents another cryostat section from liver of a mouse that received intravenous injection of a red-labeled lectin, so the sinusoidal capillary walls are revealed in red. Again, the DAPI shows liver cell nuclei in blue, and in this case, a green-labeled antibody shows the presence of albumin immunoreactivity in hepatocytes.

The avidin–biotin processed tissue also was prepared for electron microscopic study. Figure 1k presents an example of a small vessel in skeletal muscle. Arrows indicate dark positive biotinylated lectin labeling of the luminal surface of the endothelium. A portion of the endothelium from Fig. 1k is shown in greater magnification in Fig. 1l, with the arrow indicating the dark biotin labeling of the luminal surface. At this short survival period (5 min), the biotinylated lectin appears confined to the plasmalemma forming the luminal surface. Figure 1m presents a section from the liver from the same case as in Fig. 1k. The liver sinusoids are formed by an endothelium that is both fenestrated and discontinuous (Wisse 1970), and some lectins apparently were able to move from the circulating blood across the endothelium to label the hepatocyte microvilli found in the space of Disse (arrow heads).

Influence of injection parameters

The patterns of tomato lectin labeling of vascular elements vary with aspects of the injections and also with survival times after injection, as illustrated in the photomicrographs of Fig. 2. Figure 2a–c shows patterns and intensities of labeling following injections of different quantities of lectin. These animals all were injected, perfused, and tissue processed together as a cohort. Figure 2a shows only light labeling intensity with intravenous injection of 25 μg tomato lectin, while Fig. 2b shows modest labeling from
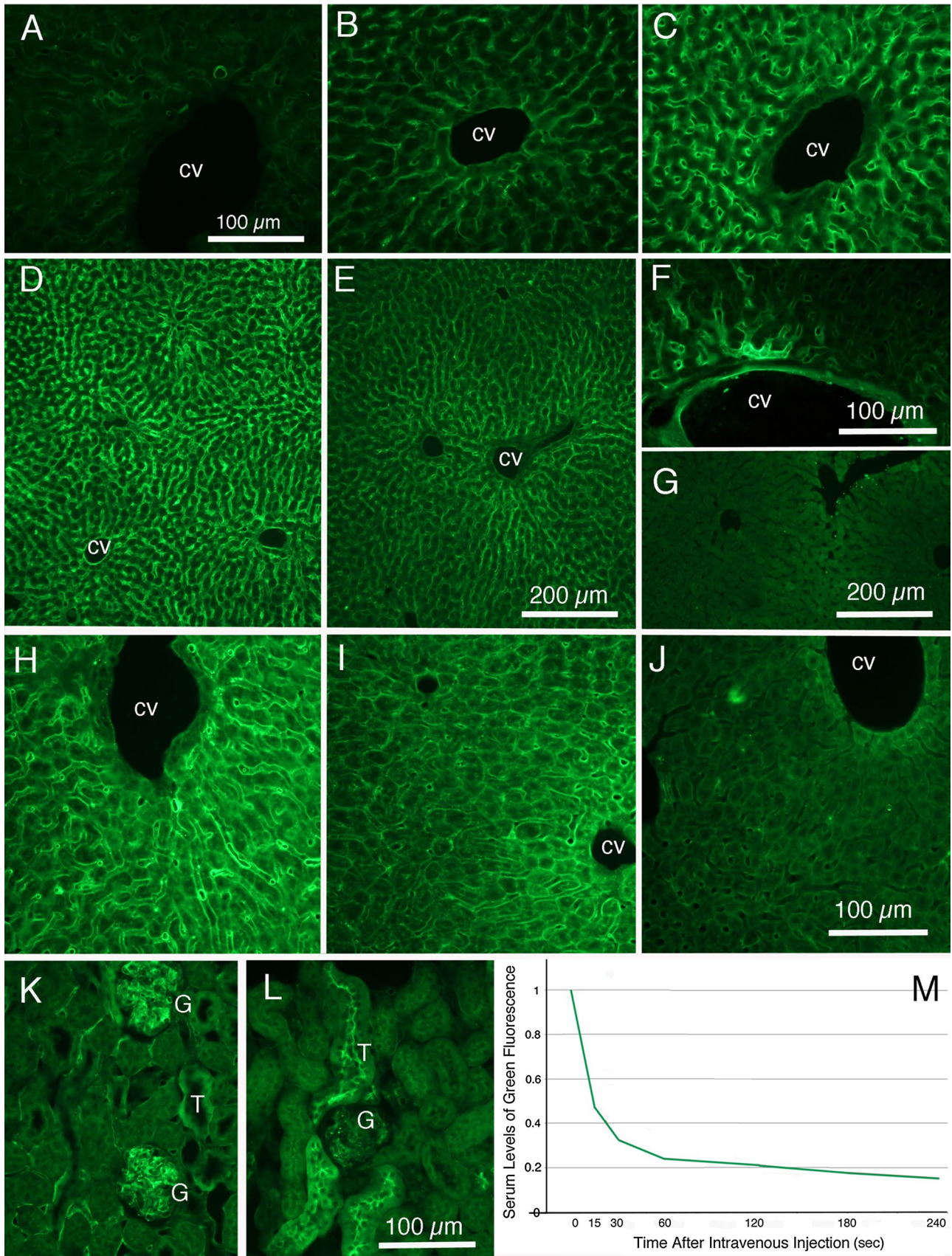
◄**Fig. 2** Lectin labeling resulting from varied experimental conditions. **a–c** Fluorescent labeling of liver following IV injection of 25 μg (**a**), 50 μg (**b**), or 100 μg (**c**) lectin. **d** Liver labeling following tail vein injection of 100 μg and 5-min survival; *cv* central venule. **e** Liver labeling following intracardiac injection of 100 μg lectin 1 min prior to saline perfusion. **f** Example of 'spotty' liver labeling following intracardiac injection. **g** Absence of liver labeling following administration of 100 μg lectin during saline perfusion. **h** Lectin labeling of liver from animal euthanized by perfusion 1 h after tail vein injection of lectin. **i** Liver labeling 4 h following lectin injection. **j** Extremely light labeling in liver 12 h after intravenous lectin injection. **k** Kidney labeling 1 h after intravenous lectin injection. **l** Kidney labeling 12 h after injection. Note very light labeling of glomeruli, and prominent labeling of convoluted tubules. **m** Graph showing rapid loss of green fluorescence in serum following tail vein injection. Ordinate presents ratio of green (lectin) fluorescence to red (control liposome) fluorescence. *Calibration bar* in **a** = 100 μm for **a**, **b**, and **c**. *Bar* in **g** = 100 μm for **e**, **f**, and **g**. *Bar* in **i** = 100 μm for **h** and **i**

injection of 50 μg lectin. Prominent labeling is shown in Fig. 2c, following injection of 100 μg lectin.

Figure 2d–g shows patterns of labeling in the liver resulting from three different injection methods. In Fig. 2d, a sedated mouse received a tail vein injection of 100 μg tomato lectin, followed by a 3-min survival period, and then vascular perfusion with saline followed by 4 % paraformaldehyde. The labeling appears excellent, both in apparent numbers of vascular elements labeled and in the intensity of labeling. Figure 2e shows an example of liver labeling from a case in which an anesthetized mouse received 100 μg lectin by an intracardiac injection, and the heart continued beating for about 1 min, followed by saline and aldehyde perfusions. The direct intracardiac injection produced strong labeling, but the labeling appeared less intense than that from tail vein injections and displayed regions of greater and lesser intensities. Figure 2f demonstrates variability of tomato lectin labeling after intracardiac injection, even within a limited region of one section of liver. Although these photomicrographs show examples of liver tissue, similar patterns of labeling were observed in all tissues studied, with the best quality of labeling resulting from intravenous injections followed by vascular perfusion after a few minutes. In a third approach, addition of 100 μg lectin in 100 μl volume to the left cardiac ventricle during the saline flush of the vasculature resulted in remarkably little vascular labeling of liver (Fig. 2g) or any other tissue.

The onset of vascular labeling by tomato lectin occurs rapidly, as documented by the photomicrographs in Fig. 2d, and also by the studies of green fluorescence clearance from serum, as shown by the graph in Fig. 2m. When measured as the ratio of green fluorescence (indicating the Dylight 488-labeled lectin) to the red fluorescence (indicating the Bodipy-labeled control liposomes, which are known to be cleared very slowly from circulating blood, Longmuir et al. 2006, 2009), the serum levels of green fluorescence appear

to have a half-life of about 15 s, and most is removed by 2 min after injection into the jugular vein.

The longevity of the labeling was studied in animals with varied post-injection survival times. As shown in Fig. 2h, k, labeling of vascular structures remains prominent at 1 h after injection of 100 μg lectin in 100 μl volume, in the liver sinusoids (Fig. 2h) and in kidney glomeruli (Fig. 2k), and in all other tissues examined. Some labeling also is seen in the secondary capillary bed of the kidney (Fig. 2k). By 4 h after injection, the intensity of labeling is decreased noticeably (Fig. 2i), and by 12 h after the injection, labeling of sinusoidal capillaries in the liver has almost disappeared (Fig. 2j). In kidney after 12 h, green lectin labeling of glomeruli has decreased remarkably, while labeling is detected in apical regions of capillary tubules (Fig. 2l). By 12 h after intravenous injection, fluorescent labeling of vasculature has almost completely disappeared from other tissues, with the exception of spleen where fluorescent label continues in the red pulp, and appears to be associated with macrophages (data not illustrated).

A possible cause of the loss of labeling could be decay in fluorescence rather than loss of lectin labeling of the vasculature. However, examination of tissue sections from animals that received tail vein injections of a cocktail mixture of fluorescently labeled tomato lectin and biotinylated lectin revealed similar declines of labeling intensity, as indicated by comparable fluorescence detection and by biotin histochemistry (data not illustrated).

Discussion

Techniques of administering lectins

Several investigators have applied lectins to fixed tissue sections (Nag 1985; Jilani et al. 2003; Mazzetti et al. 2004; Baratta et al. 2009) and have successfully labeled capillaries and other small vascular elements. Indeed, it was initially the positive results achieved on tissue sections (Baratta et al. 2009) that prompted our interest in the use of intravascular administration in the living animal. The quality of the results appears to be impacted strongly by injection parameters. Intravascular injections in vivo, followed by short post-injection survival periods, produced images with the finest details and brightest fluorescence (Lee et al. 2002; Gee et al. 2003; Inai et al. 2004; present results). An injected dose of 100 μg of lectin in 100 μl volume resulted in the best results, as indicated by the relative brightness and clarity of labeling. Short post-injection survival times also include the very short times that are associated with direct intracardiac injections just before perfusions (Huang et al. 2003). This technique is likely to be useful in studies of development of vasculature in late fetal or newborn

animals, in which intravenous injections would be particularly challenging. Further, intracardiac injections in living animals that would be intended to survive for some time after the injection could be efficacious for those with the technical skills and institutional approval to perform these procedures.

Several different lectins have been used experimentally by several groups of investigators (Simionescu et al. 1982; Nag 1985; Alroy et al. 1987; Debbage et al. 1998; Jilani et al. 2003). Differences in results from different lectins were reported, but overall, the tomato lectin appears to provide consistently strong labeling. Further, tomato lectin appears to be the best candidate for studies of central nervous system (CNS) vasculature, as use of other lectins reportedly produces poor labeling of CNS vasculature (Debbage et al. 1998).

In an earlier study, Simionescu et al. (1982) achieved vascular labeling by first flushing the vascular system with buffered saline and then perfusing with one of several lectins. Tomato lectin was not among the lectins tested. Although these authors report labeling of vascular structures, our attempts to achieve labeling by tomato lectin perfusion following a vascular flush with PBS were only marginally successful. Perhaps a greater quantity of lectin, or a different lectin, is required.

Specificity of labeling

Morphological features of the fluorescent or biotin labeling strongly suggest that it is endothelial cells that are being labeled by the injected tomato lectin. This suggestion is supported by demonstrations of the correspondence of lectin labeling and other markers of endothelial cells including immunoreactivity to CD31 (Gee et al. 2003; Inai et al. 2004). Most relevant, our electron microscopic studies reveal the presence of biotin-labeled lectin on the luminal surface of endothelial cells (Fig. 1).

Several lectins, including the tomato lectin used in the present studies, bind to glycoconjugates associated with the plasmalemma of endothelial cells. Analyses using lectin blot analyses or affinity chromatography have revealed that the *LEA* (tomato lectin) binds to complex-type *N*-glycans glycoproteins, particularly the poly-*N*-acetyllactosamine residues of complex carbohydrates (Kawashima et al. 1990; Nachbar et al. 1980; Oguri 2005; Zeng et al. 1998) including oligosaccharide sequences that contain the i and l—antigenic structures (Kawashima et al. 1990). Tomato lectin binds also to glycoproteins containing high mannose-type *N*-glycans.

The glycoproteins to which the tomato lectin is binding likely serve a variety of functions (Rutishauser and Sachs 1975) for endothelial cells, including interactions with plasma proteins and leukocytes. Because these carbohydrate ligands are found on the luminal surface of capillary endothelial cells, they provide an easily accessible target for lectins in circulating blood and hence offer a simple method for visualizing morphological features of capillary beds.

The presence of these glycoprotein-binding sites on endothelial cells implicates the presence of endogenous molecules including the galectins or cells with which the binding sites normally would interact (Debbage et al. 1988). Thus, the experimentally applied lectin may in some normal, pathological, or experimentally altered condition compete with those endogenous molecules or cells for access to the binding sites. These endogenous competing molecules or cells thus may lead to variation in intensity of lectin binding in experimental studies.

While this binding provides a useful marker when applied to fixed tissue sections (Nag 1985; Mazzetti et al. 2004; Baratta et al. 2009), it also is compatible with intravascular delivery of the lectin, where intravascular administration allows direct exposure of the tomato lectin to the luminal endothelial surface. If lectin is applied following fixation (Simionescu et al. 1982), affinity of binding may be reduced due to aldehyde-induced alterations of the glycoprotein-binding sites, leading to somewhat reduced labeling. However, aldehyde fixation dos not eliminate tomato lectin labeling as evidenced by the labeling that results from relatively long (1–2 h) incubations of lectin on tissue slices (Baratta et al. 2009).

Other studies report evidence for selectivity of labeling by some lectins (Alroy et al. 1987; Jilani et al. 2003). Interestingly, Debbage et al. (1998) report that CNS labeling is not achieved from use of other lectins, suggesting that the tomato lectin may be particularly advantageous in studies of CNS vasculature (Mazzetti et al. 2004).

The extensive labeling of vasculature by intravenously applied tomato lectin also opens the possibility of revealing extensive and detailed three-dimensional images of the vasculature of any organ through use of new techniques of tissue clearance (Ertürk et al. 2012; Chung et al. 2013; Renier et al. 2014).

Temporal aspects of tomato lectin binding

The binding of tomato lectin to endothelial cells apparently occurs quite rapidly. Our analysis of fluorescence in circulating blood serum suggests that the half-life of the green fluorescent-labeled lectin in circulating blood is about 15 s (Fig. 2j) and is largely cleared within 1–2 min. These blood clearance data indicate that the tomato lectin is removed from circulating blood significantly faster than clearance time for nanoparticles that are taken up by the reticuloendothelial system of the liver, spleen, and other organs (Simon et al. 1995). The present results demonstrating

rapid lectin clearance from blood are in agreement with our findings that labeling of vascular elements occurs within 1 min following direct intracardiac injections of lectins.

Following intravenous injection, the circulating lectin would first encounter the capillary bed in lung and then subsequently through peripheral circulation to the capillary beds of other tissues and organs. Calculations of mouse blood circulation suggest that lectin in the serum would reach major organs within 10 s (Janssen et al. 2002), a figure in line with a recent report that intravenously applied carbon nanotubes can be detected in brains of living mice within a few seconds (Hong et al. 2014). Further, our observation that extensive labeling of capillary beds resulting from direct intracardiac injections of lectin followed within 1 m with vascular perfusion, also support the notion of rapid binding to endothelium.

The rapid clearing of lectin from circulating blood is comparable to rapid clearance of other dyes (Trotter et al. 1989) and also with other reports that intravascular injection of Evans blue results in generalized body staining within 15 s (Debbage et al. 1998). Clearance from blood is probably due to a combination of endothelial binding, uptake by the reticulo-endothelial system, some tissue extravasation, and renal clearance. The present studies support the idea that renal clearance plays a role in the decline in serum levels of the lectin. Shortly after intravenous injection, kidney glomeruli are strongly labeled; later, fluorescence can be detected in the apical regions of convoluted tubules in kidney cortex, suggesting the lectin has moved through the filtration barrier of the kidney glomeruli and is, in part, undergoing some reuptake by kidney convoluted tubules.

Tomato lectin labeling of endothelial cells appears to slowly decline over several hours following intravenous administration, supporting the conclusions of other investigators using other lectins (Debbage et al. 1998). The mechanisms of the loss of labeling are not entirely clear, but because glycoproteins of the endothelial plasma membrane normally undergo recycling, protein digestion may lead to release of the fluorescent or biotin marker and hence the reduction of detectable labeling. This decline over hours in labeling suggests that one-time administration may not be appropriate for studies of the response of vascular elements over time, for example, following experimentally induced injury or response to stimulation. However, the rate of disappearance may vary from region to region, depending on subtypes of endothelial cells.

Conclusions

Capillary labeling by tomato lectin is widely distributed following intravascular injections. Clear labeling of capillaries was observed in every tissue examined, including brain, liver, spleen, kidney, small intestine, heart, and skeletal muscle. Intravascular administration of tomato lectin appears to be a sensitive and reliable method of visualizing vascular structures, and particularly capillaries, in a variety of tissues and organs.

References

Alroy J, Goyal V, Skutelsky E (1987) Lectin histochemistry of mammalian endothelium. Histochemistry 86:603–607

Baluk P, McDonald DM (2008) Markers for microscopic imaging of lymphangiogenesis and angiogenesis. Ann N Y Acad Sci 1131:1–12

Baratta JL, Ngo A, Lopez B, Kasabwala N, Longmuir KJ, Robertson RT (2009) Cellular organization of normal mouse liver: a histological, quantitative immunocytochemical, and fine structural analysis. Histochem Cell Biol 131:713–726

Barondes SH (1988) Bifunctional properties of lectins: lectins redefined. Trends Biochem Sci 13:480–482

Chung K, Wallace J, Kim S-Y, Kalyanasundaram S, Andalman AS, Davidson TJ, Mirzabekov JJ, Zalocusky KA, Mattis J, Denisin AK, Pak S, Bernstein H, Ramakrishnan C, Grosenick L, Gradinaru V, Deisseroth K (2013) Structural and molecular interrogation of intact biological systems. Nature 497:332–337

Debbage PL, Gabius HJ, Bise K, Marguth F (1988) Cellulara glycoconjugates and their potential endogenous receptors in the cerebral microvasculature of man: a glyocohistochemical study. Eur J Cell Biol 46:425–534

Debbage PL, Griebel J, Reid M, Gneiting T, DeVries A, Hutzler P (1998) Lectin intravital perfusion studies in tumor-bearing mice: micrometer-resolution, wide-area mapping of microvascular labeling, distinguishing efficiently and inefficiently perfused microregions in the tumor. J Histochem Cytochem 46:627–639

Ertürk A, Becker K, Jährling N, Mauch CP, Hojer CD, Egen JG, Hellai F, Bradke F, Sheng M, Dodt H-U (2012) Three-dimensional imaging of solvent-cleared organs using 3DISCO. Nat Protoc 7:1983–1995

Fina L, Molgaard HV, Robertson D, Bradley NJ, Monaghan P, Delia D, Sutherland DR, Baker MA, Greaves MF (1990) Expression of the CD34 gene in vascular endothelial cells. Blood 75:2417–2426

Gee MS, Procopio WN, Makonnen S, Feldman MD, Yeilding NM, Lee WM (2003) Tumor vessel development and maturation impose limits on the effectiveness of anti-vascular therapy. Am J Pathol 162:183–193

Hashizume H, Baluk P, Morikawa S, McLean JW, Thurston G, Roberge S, Jain RK, McDonald DM (2000) Openings between defective endothelial cells explain tumor vessel leakiness. Am J Pathol 156:1363–1380

Hong G, Diao S, Chang J, Antaris AL, Chen C, Zhang B, Zhao S, Atochin DN, Huang PL, Andreasson K, Kuo CJ, Dai H (2014) Through-skull fluorescence imaging of the brain in a new near-infrared window. Nat Photonics 8:723–730

Huang JZ, Frischer JS, Serur A, Kadenhe A, Yokoi A, McCrudden KW, New T, O'Toole K, Zabski S, Rudge JS, Holash J,

Yancopoulos GD, Yamashiro DJ, Kandel JJ (2003) Regression of established tumors and metastases by potent vascular endothelial growth factor blockade. Proc Natl Acad Sci USA 100:7785–7790

Inai T, Manusco M, Hashizume H, Baffert F, Haskell A, Baluk P, Hu-Lowe DD, Shalinsky DR, Thurston G, Yancopoulos GD, McDonald DM (2004) Inhibition of vascular endothelial growth factor (VEGF) signaling in cancer causes loss of endothelial fenestrations, regression of tumor vessels, and appearance of basement membrane ghosts. Am J Pathol 165:35–52

Janssen B, Debets J, Leenders P, Smits J (2002) Chronic measurement of cardiac output in conscious mice. Am J Physiol Regul Integr Comp Physiol 282:R928–R935

Jilani SM, Murphy TJ, Thai SN, Eichmann A, Alva JA, Iruela-Arispe ML (2003) Selective binding of lectins to embryonic chicken vasculature. J Histochem Cytochem 51:597–604

Kawashima H, Sueyoshi S, Li H, Yamamoto K, Osawa T (1990) Carbohydrate binding-specificities of several poly-*N*-acetyllactosamine-binding lectins. Glycoconj J 7:323–334

Lee JC, Kim DC, Gee MS, Saunders HM, Sehgal CM, Feldman MD, Ross SR, Lee WM (2002) Interleukin-12 inhibits angiogenesis and growth of transplanted but not in situ mouse mammary tumor virus-induced mammary carcinomas. Cancer Res 62:747–755

Lokmic Z, Mitchell GM (2011) Visualisation and stereological assessment of blood and lymphatic vessels. Histol Histopathol 26:7781–7796

Longmuir KJ, Robertson RT, Haynes SM, Baratta JL, Waring AJ (2006) Effective targeting of liposomes to liver and hepatocytes in vivo by incorporation of a Plasmodium amino acid sequence. Pharm Res 23:759–769

Longmuir KJ, Haynes SM, Baratta J, Kasabwala N, Robertson RT (2009) Liposomal delivery of doxorubicin to liver and hepatocytes in vivo by targeting hepatic heparan sulfate glycosaminoglycan. Int J Pharmaceut 382:222–233

Mazzetti S, Frigerio S, Gelati M, Salmaggi A, Vitellaro-Zuccarello L (2004) *Lycopersicon esculentum* lectin: an effective and versatile endothelial marker of normal and tumoral blood vessels in the central nervous system. Eur J Histochem 48:423–428

Nachbar MS, Oppenheim JD, Thomas JO (1980) Lectins in the U.S. Diet. Isolation and characterization of a lectin from the tomato (*Lycopersicon esculentum*). J Biol Chem 255:2056–2061

Nag S (1985) Ultrastructural localization of lectin receptors on cerebral endothelium. Acta Neuropathol (Berl) 66:105–110

Newman PJ, Albelda SM (1992) Cellular and molecular aspects of PECAM-1. Nouv Rev Fr Hematol 34(Suppl):S9–S13

Oguri S (2005) Analysis of sugar chain-binding specificity of tomato lectin using lectin blot: recognition of high mannose-type *N*-glycans produced by plants and yeast. Glycoconj J 22:453–461

Renier N, Wu Z, Simon DJ, Yang J, Ariel P, Tessier-Lavigne M (2014) iDISCO; A simple, rapid method to immunolabel large tissue samples for volume imaging. Cell 159:896–910

Robertson RT, Baratta JL, Haynes SM, Longmuir KJ (2008) Liposomes incorporating a plasmodium amino acid sequence target heparin sulfate binding sites in liver. J Pharm Sci 97:3257–3273

Rutishauser U, Sachs L (1975) Cell-to-cell binding induced by different lectins. J Cell Biol 65:247–257

Simionescu M, Simionescu N, Palade GE (1982) Differentiated microdomains on the luminal surface of capillary endothelium: distribution of lectin receptors. J Cell Biol 94:406–413

Simon BH, Ando HY, Gupta PK (1995) Circulation time and body distribution of ^{14}C-labeled amino-modified polystyrene nanoparticles in mice. J Pharm Sci 84:1249–1253

Smolkova O, Zavadka A, Bankston P, Lutsyk A (2001) Cellular heterogeneity of rat vascular endothelium as detected by HPA and GS I lectin-gold probes. Med Sci Monit 7:659–668

Trotter MJ, Chaplin DJ, Olive PL (1989) Use of a carbocyanine dye as a marker of functional vasculature in murine tumours. Br J Cancer 59:706–709

Wisse E (1970) An electron microscopic study of the fenestrated endothelial lining of rat liver sinusoids. J Ultrastruct Res 31:125–150

Zeng X, Murata T, Kawagishi H, Usui T, Kobayashi K (1998) Analysis of specific interactions of synthetic glycopolypeptides carrying *N*-acetyllactosamine and related compounds with lectins. Carbohydr Res 312:209–217